Photoemission spectra from conduction bands and core levels of sputter-deposited tungsten films

Claude M. Penchina* and Edwin Sapp*
Department of Physics and Astronomy, University of Massachusetts, Amherst, Massachusetts 01002

Javier Tejeda and Nigel Shevchik
Max-Planck-Institut für Festkörperforschung, Stuttgart, Federal Republic of Germany
(Received 23 January 1974; revised manuscript received 6 May 1974)

Photoemission spectra of tungsten films, deposited by sputtering onto a room-temperature substrate, were obtained using an aluminum x-ray source (Al $K\alpha_{1,2}$ −1486.6 eV) and a helium uv resonance lamp (He I, 21.2 eV and He II, 40.8 eV). Film structure was determined by x-ray diffraction to consist mostly of bcc microcrystals. Spectra of electrons excited from the conduction band by x rays (XPS) and uv (UPS) are combined to deduce a high-resolution empirical density of electron states of the conduction band. The 10-eV Fermi energy agrees well with augmented-plane-wave calculations if relativistic effects and exchange are appropriately taken into account. The XPS data, when calibrated by the high-resolution UPS data with respect to the Fermi energy, provide accurate core-level binding energies. They also show electron energy losses due to 25-eV volume plasmon excitation.

I. INTRODUCTION

A wide variety of experimental investigations on high-purity single-crystal body-centered-cubic tungsten (see references in introduction of Ref. 1) encouraged several recent band-structure and Fermi-surface computations.[1-5] These computations all use some variation of the augmented-plane-wave (APW) method,[6] but each with its own modifications, such as variation of the exchange energy,[1] or inclusion of relativistic effects.[3,4] The results are qualitatively the same, and differ mainly in the energy scale. They show the conduction bands below the Fermi energy to be composed essentially of 5*d* and 6*s* orbitals with a possible small contribution (Ref. 1, *E*2 calculation) from 6*p* electrons near the Fermi surface. There are six conduction electrons per atom. The Fermi energy is computed to be about 6.5–10.3 eV above the bottom of the 6*s* conduction band. The 5*d* conduction band overlaps with the 6*s*, but its bottom is about 0.95–1.25 eV higher.

Recently, uv photoemission measurements on polycrystalline tungsten foils[7] and oriented single crystals[8] have shown qualitative agreement with the band-structure calculations and have been used to study effects of contamination by carbon, oxygen, and carbon monoxide.

Chopra *et al.*[9,10] showed that, by appropriate temperature control, thick films of tungsten could be prepared in amorphous form or face-centered-cubic crystalline form, as well as the usual bcc crystalline form. They used a very low (10^{-5} Torr) argon pressure during sputtering. Transmission electron diffraction measurements on amorphous tungsten showed lines so broad that one could not tell if it had a structure closer to the fcc phase or the bcc phase. Sella and Coppens[11] have also obtained the amorphous and fcc phases at a higher pressure (10^{-3} Torr). No band-structure computations have been published for either the fcc or amorphous phases.

In the present paper, we study a combination of x-ray-induced (XPS) and uv-induced (UPS) photoelectron spectra of sputtered tungsten. The XPS and UPS measurements have rather different character, and provide very useful complementary information.

The high energy (1486.6 eV) of the x rays permits electrons to escape from deeper in the film than electrons excited by the He uv lamp (see the "universal curve" of escape depths[12]). Also the cross section for photoelectric excitation of the outer electrons of oxygen is much smaller for XPS than for UPS. Thus, XPS should be much less sensitive to surface contamination than UPS, a result borne out by our experiments on contaminated surfaces.[13] Because little structure exists in the density of electron final states at high energy, the energy distribution of emitted electrons reflects primarily the structure in the filled states. With a nonmonochromatized x-ray source, resolutions of only 1.2 eV are obtainable (1.5 eV with the larger analyzer slit used for weak signals), and the presence of the $K\alpha_{3,4}$ lines[14] (~1496 eV) limits its use to study of the conduction band of materials lacking core levels close to it. In tungsten, the core levels are sufficiently separated from the conduction band that no problem is caused by these satellite lines. With monochromatized x rays, a resolution of about 0.5 eV can be obtained, and the satellite lines are eliminated.

High resolution (0.1 eV for He I and 0.2 for He II) UPS measurements are used[15] to improve the accuracy of the XPS measurements by accurately locating a common reference point, in this case the Fermi energy. The smaller escape depth of the uv excited electrons, while making it more difficult to study bulk effects in clean samples, makes it easier to study the effects of contamination on the surface.

The Fermi energy in the XPS data is located by taking into account the instrumental broadening at the Fermi edge and shifting the curves for a best fit to the UPS data. This procedure takes account of any errors such as shifts in the effective analyzer work function due to use of different analyzer slits for different photon energies.

II. EXPERIMENT

The measurements (with the exception of those of Fig. 4 which used an HP system as described in Sec. III B) were performed with a Vacuum Generators ESCA III system, equipped with an x-ray source and a differentially pumped He lamp, at a base pressure of 2×10^{-9} Torr or better, even when the He lamp is on. Samples (~0.5 μm thick) were prepared inside the sample preparation chamber (turbomolecular pumped, base pressure 10^{-7} Torr) of the system by diode sputtering of tungsten onto a stainless-steel substrate at room temperature in an argon atmosphere (10^{-6} purity) at 3×10^{-2} Torr with a dc current of 2 mA at 2300 V. The argon was pumped out and, without breaking the vacuum, the sample was moved to the analyzer chamber. The sample was then maintained in ultrahigh vacuum (better than 2×10^{-9} Torr) throughout the measurements.

The sputtering target was a polycrystalline tungsten foil, 99.95+% pure, obtained from R. D. Mackay Co. The major trace impurities in the foil were expected to be[16] Na, Si, and K. Also, one might expect to find argon as an impurity in the sputter-deposited film. However, no spectral lines characteristic of these impurities were observed with the sensitivity obtainable in our XPS measurements. On the other hand, we did see an oxygen 1*s* XPS line which varied in strength from sample to sample, presumably due to surface contamination (as will be documented more fully in the discussion of the conduction bands). We classify sample surface contamination by the height of the oxygen 1*s* line relative to the strong tungsten $4f_{7/2}$ line, henceforth to be called the oxygen contamination ratio. In the discussion of conduction bands, it is shown that an oxygen contamination ratio of 3% corresponds to roughly one monolayer of surface oxygen. Only the "dirtiest" of our samples showed a carbon 1*s* XPS line. This sample, which had an oxygen contamination ratio of 27%, also had a carbon contamination ratio of 20%. All other samples had a carbon 1*s* line smaller than a plasmon peak which occurs at the same voltage; thus, an upper bound to the carbon contamination ratio was 1% for all but one sample, where it was 20%.

It has been shown by Nagata and Shoji[17] that the fcc structure seen by Chopra *et al.*[10] on Mo was really γ-Mo_2N. Thus, we decided to determine the structure of our W films by x-ray diffraction. We prepared thicker films (~4 μm) of W under similar conditions on both glass and copper substrates. The diffraction pattern on these thick films shows all the peaks that correspond to the bcc lattice. Their broadness at high angles and the high background indicated a microcrystalline (10–20 Å) structure. We also observe some of the features seen by Chopra[10] and identified to be fcc and amorphous tungsten. Since all our samples were much thicker than the 10–20-Å microcrystals, the effect of different substrates and thicknesses could not be very important. Thus, we conclude that the thinner samples used for photoemission had essentially the same structure as the thicker ones used for x-ray diffraction.

III. RESULTS

A. Sensitivity to surface contamination

UPS and XPS data for excitation of conduction-band electrons from various samples are shown in Figs. 1–3. Examination of Figs. 1 and 2 shows that the major effect on UPS of increased oxygen contamination is an increase in the 3-eV-wide peak centered about 6 eV below the Fermi energy. This peak is larger with 40.8-eV excitation than with 21.2-eV excitation. Previous studies of the effects of oxygen contamination on clean [110] surfaces of bcc tungsten[8] showed a very similar peak, which was stronger for 21.2-eV excitation than for 16.8-eV excitation.

If we assume that surface oxygen looks similar on crystalline and sputtered tungsten, we can compare our 21.2-eV excitation data of Fig. 1 with those of Baker.[8] This comparison indicates that our cleanest sample (A) with 1% oxygen contamination ratio, had about $\frac{1}{3}$ monolayer of oxygen on the surface, and that sample (B), for which the ratio was 4%, had about $\frac{4}{3}$ monolayers of oxygen. Assuming this approximate linearity continues to higher surface coverage, we would find that the sampled volume of (C), our dirtiest sample, was mostly oxidized since it shows the equivalent of nine monolayers of oxygen, along with a fairly large amount of carbon. (These estimates also agree with estimates from comparison of the XPS

oxygen 1s signal with that from oxygen 1s in SiO_2.[18])

XPS data on the conduction-band electrons (Fig. 3) show that an increase from $\frac{1}{3}$ to $\frac{4}{3}$ monolayers of oxygen has a negligible effect on the spectrum. However, nine monolayers of oxygen, together with some carbon, show the 6-eV oxygen peak appearing (unresolved) as a large plateau on the energy distribution curve.

The trend of sensitivity to surface contamination observed in both our experiments and Baker's is in agreement with that predicted by the "universal curve" of escape depths[12]; i.e., the escape depth decreases from 16.8- to 40.8-eV excitation, but then increases considerably for 1486.6-eV excitation. Changes in the photoionization cross sections with photon energy can also alter the sensitivity to contamination. We expect the oxygen L shell to have a higher cross section in the uv region than the tungsten O and P shells.[13]

B. Density of conduction states

From a critical examination of Figs. 1–4, we can put together a composite picture of an empirical density of states for the conduction band below the Fermi energy E_F. We start with a discussion of states near E_F and then move in the direction of tighter binding.

For the first 4 eV below E_F, the UPS spectra are essentially independent of oxygen contamination, and are of high resolution. The electronic states involving the oxides as a rule lie 3–5 eV deeper in energy. In general, one would expect some influence of the final states density on the UPS spectra. However, comparison of the curves for He I (Fig. 1) and He II (Fig. 2) excitation shows that for the first electron volt, they are almost identical. Thus, the effect of the density of final states is indeed small, and we use the high-resolution UPS data instead of the lower-resolution XPS data over this 1-eV energy range. For the next 3 eV, the He II data are quite similar to the XPS data (Fig. 3) on the cleaner samples, thus indicating that there is no fine structure in the density of states in this range which is missed due to the low resolution of XPS. Thus, we can use either the XPS or the very similar He II UPS data from 1 to 4 eV below E_F.

From 4 to 8 eV below E_F, the UPS data are strongly influenced by even small oxygen contamination. Thus, here we have to use the XPS data directly, and cannot make use of UPS data to improve resolution. We can, however, deconvolute the XPS data with a 0.5-eV Lorentzian to remove part of the 1.5-eV broadening, a combination of the x-ray linewidth and instrumental resolution. However, attempts to obtain higher resolution by deconvoluting the data with a broader Lorentzian

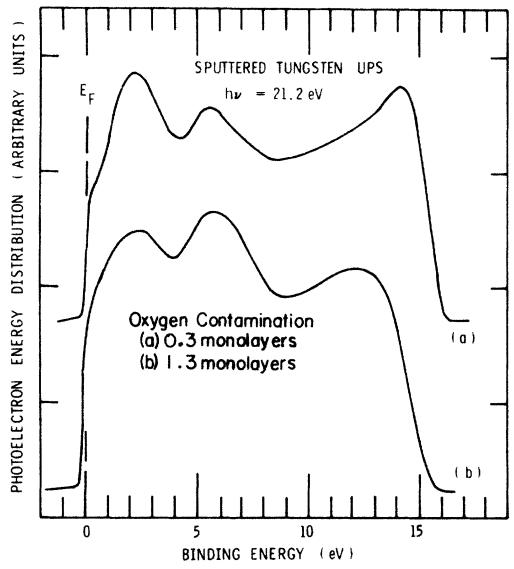

FIG. 1. Energy distribution curves of photoelectrons from sputtered tungsten excited by He I ultraviolet-light source ($h\nu$=21.2 eV). The energy scale is photon energy minus measured photoelectron energy relative to the Fermi level as reference. For unscattered photoelectrons, this corresponds to the binding energy (below the Fermi energy) of the initially filled electron states. Curves are offset vertically for clarity, but have the same vertical sensitivity.

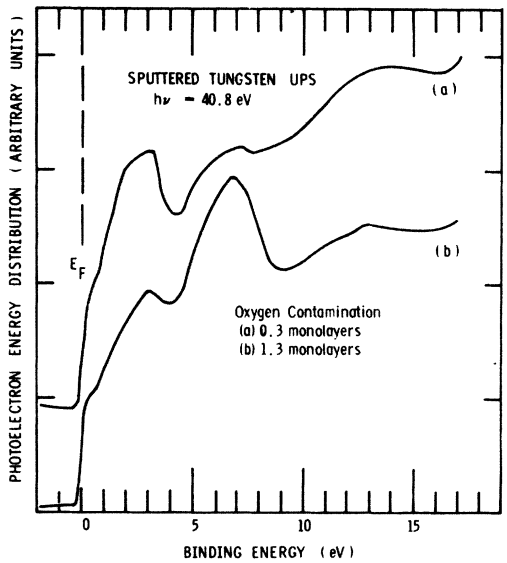

FIG. 2. Energy distribution curves of photoelectrons from sputtered tungsten excited by He II ultraviolet-light source ($h\nu$=40.8 eV). The energy scale is photon energy minus measured photoelectron energy relative to the Fermi level as reference. For unscattered photoelectrons, this corresponds to the binding energy (below the Fermi energy) of the initially filled electron states. Curves are offset vertically for clarity, but have the same vertical sensitivity.

function lead to nonphysical results due to noise in the original data. Thus, to improve resolution in this range, we prepared a sample the same way (but with base pressure of 10^{-6} Torr in the sample preparation chamber) in a Hewlett Packard ESCA system. This system uses an x-ray monochromator to achieve an over-all resolution of about 0.5 eV (see Fig. 4) and to eliminate x-ray satellites. However, the sample obtained had about three monolayers of oxygen, thus preventing us from using these higher-resolution data in the desired 4–8-eV energy region. The elimination of satellites turns out to be important, as discussed below.

Beyond 8 eV below E_F, data from all three excitation energies show a broad more-or-less structureless region which presumably is due to emission of electrons which suffer inelastic scattering after photoexcitation, rather than from unscattered primary photoelectrons. This would be expected from theoretical band-structure calculations which show the bottom of the conduction band extending to a depth of 6.5–10.3 eV from E_F, with a rather low density of states in the deepest 1–2 eV.

The XPS spectra of Fig. 3 and the He II UPS spectra of Fig. 2 show additional weak broad structure about 12 eV from E_F, 9 eV from the peak. At first it was thought that this might indicate a 9-eV energy loss[19-22] due to excitation of a surface plasmon[21] shifted to lower energy because of the microcrystalline structure[23] of our samples, or due to a single-particle excitation. The extra structure is no longer present in the monochromatized XPS data of Fig. 4, showing that it was not a 9-eV energy loss, but due instead to photoelectrons excited from the $4f$ and the $5p_{3/2}$ core states by the weak $K\alpha_{5,6}$ satellites at 20.6 and 24.0 eV higher energy, respectively, than the center of the main $K\alpha_{1,2}$ x-ray line[14]; the monochromator eliminates these satellites and clearly brings out the density of electron states from 8–10 eV below E_F.

Thus, the structure from 9–16 eV below E_F in the He II UPS spectra is most likely due to electrons emitted 25–32 eV above the Fermi energy by an Auger process involving the $4f$ and $5p_{3/2}$ core levels, and the filled states in the conduction band. The structure around 13–14-eV binding energy in the data taken with $h\nu = 21.2$ eV (Fig. 1) is simply a combination of a rapidly rising background of low-energy inelastically scattered secondary electrons (which obscures any possible real structure) and a cutoff due to the work function of the surface. The cutoff at 16.2 eV for the cleanest sample indicates that the work function of sputtered tungsten is 5.0 eV. As might be expected, this is between the previously reported value of 4.4[7]–4.6[24] eV for clean (100) surfaces and

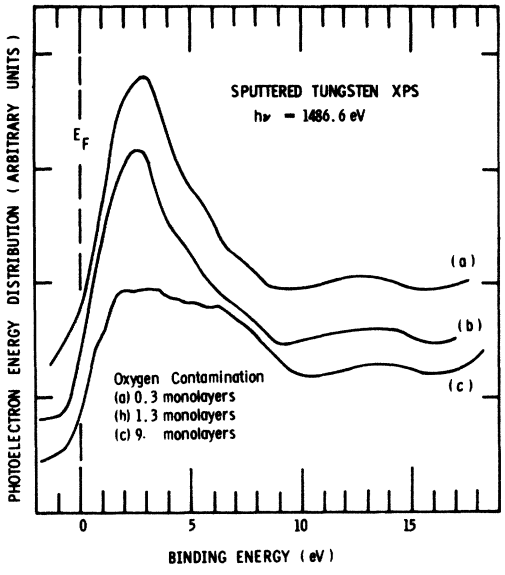

FIG. 3. Energy distribution curves of photoelectrons from sputtered tungsten excited by Al $K\alpha_{1,2}$ x-ray source ($h\nu = 1486.6$ eV). The energy scale is photon energy minus measured photoelectron energy relative to the Fermi level as reference. For unscattered photoelectrons, this corresponds to the binding energy (below the Fermi energy) of the initially filled electron states. Curves are offset vertically for clarity, but have the same vertical sensitivity.

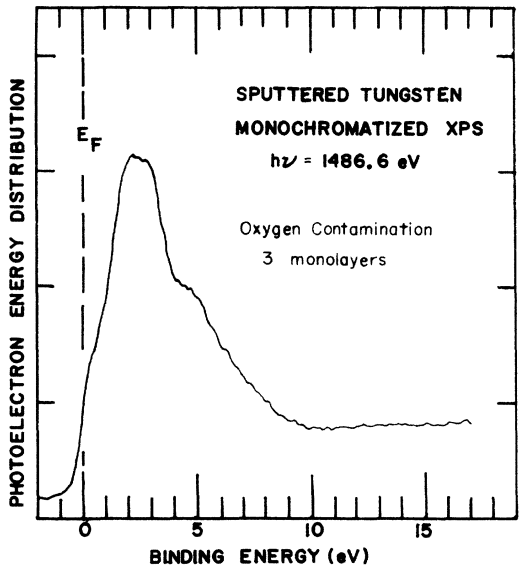

FIG. 4. Energy distribution curves of photoelectrons from sputtered tungsten excited by monochromatized Al $K\alpha$, x-ray source ($h\nu = 1486.6$ eV). The energy scale is photon energy minus measured photoelectron energy relative to the Fermi level as reference. For unscattered photoelectrons, this corresponds to the binding energy (below the Fermi energy) of the initially filled electron states.

5.25 eV[24] for clean (110) surfaces.

We extrapolate the inelastically scattered electron contribution back to E_F and subtract it from the total measured energy distribution curves (EDC) to obtain the contribution from unscattered primary photoelectrons.

Thus, we are led to the empirical conduction-band density of states of sputtered tungsten shown in Fig. 5. To summarize our procedure, this empirical curve was obtained from our cleanest sample by using UPS data from 0–1 eV, He II UPS data and XPS data from 1–4 eV, deconvoluting out some of the instrumental linewidth from the nonmonochromatized XPS data from 4–8 eV, using monochromatized XPS data to eliminate effects of satellite lines from 8–10 eV, and subtracting the contribution of inelastically scattered electrons.

For comparison, in Fig. 5 we show one theoretical density of states[5] for crystalline bcc tungsten along with our empirical density of states for sputtered tungsten. It should be noted in this comparison that, when different variations on the APW method are used, the shape of the theoretical curve remains nearly constant but its energy scale expands or contracts. The Fermi energy is found to be 10 eV above the bottom of the conduction band. This is larger than the value found in standard nonrelativistic APW treatments. However, Loucks[4] relativistic calculation (RAPW) predicts a Fermi energy of 10.3 eV, and Mattheiss's nonrelativistic E_2 calculation[1] in which the Slater[6] exchange is reduced by 30% predicts 9.5 eV; both values are in fairly good agreement with our experiment.

The empirical density of states for sputtered tungsten shows some broadening and some shifts relative to the EDC's of crystalline tungsten. However, these differences are of the same order of magnitude as the differences found for crystalline tungsten itself when the uv excitation energy is changed or the orientation of the crystal is changed.[7,8]

C. Core levels

Figure 6 shows a wide-scan energy distribution spectrum for Al $K\alpha$ excitation of sputtered tungsten. The spectral structure is identified by comparison with the energy levels expected for crystalline tungsten.[25] This, however, leaves some ambiguity in the identification of the N_{VI}, N_{VII}, and O_{III} levels. The spectral region of interest is shown enlarged in Fig. 7. Owing to the different degeneracies of the states, one expects the O_{III} ($5p_{3/2}$) signal to be twice as strong as the O_{II} ($5p_{1/2}$) signal. However, since the O_{II} signal in Fig. 6 is so weak relative to the doublet seen in Figs. 6 and 7, we expect that the O_{III} would be lost in this doublet. Hence, we attribute the strong doublet to N_{VI} ($4f_{5/2}$) and N_{VII} ($4f_{7/2}$) which, in fact, do appear in Fig. 7 with the relative strengths corresponding to their relative statistical weights of 6 : 8. (In Fig. 6, these strengths are distorted due to a time-constant effect.) In Table I, we list a comparison of our core-level binding energies with those tabulated by Bearden and Burr.[25]

Within the uncertainties quoted, all the shifts could almost fit 2.1 eV. However, it is apparent that the d and f levels seem to be shifted considerably more than the s and p levels. The average shift of the d and f levels is 2.1 eV and the average of the s and p shifts is 0.9 eV. There is an over-all uncertainty in the shifts due to the uncertainty in the calibration level used by Bearden and Burr. For example, they list the carbon 1s binding energy as 283.8 ± 0.4 eV for pure carbon, whereas more recent[26] determinations indicate that it is 284.3 ± 0.3 eV for graphite and for amorphous carbon and 285.0 ± 0.4 eV for carbon contamination from diffusion pump oil.[27] In addition, as will be noted in our discussion of contamination effects on the core-level XPS spectrum, there is some possibility that there may be some contamination effects in the data on which Bearden and Burr's tabulated levels are based. Thus, although we believe that our quoted binding energies for

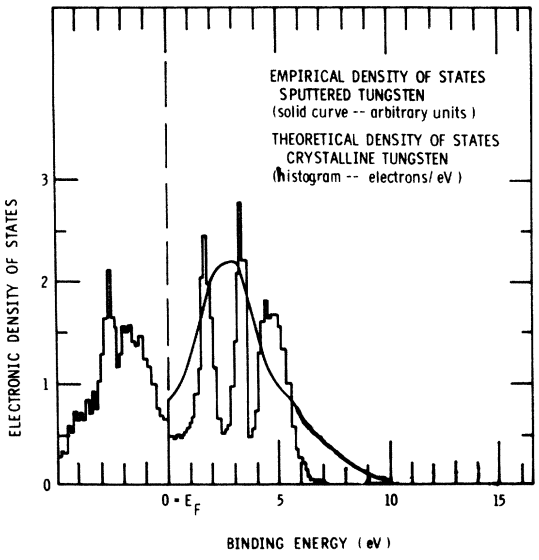

FIG. 5. Curve is the empirical density of states for sputtered tungsten deduced from our UPS and XPS measurements. The resolution is 0.1 eV from 0–1 eV, 0.2 eV from 1–4 eV, 1.0 eV from 4–8 eV, and 0.5 eV from 8–10 eV. The histogram is a theoretical density of states for bcc crystalline tungsten from Petroff (1971) (Ref. 5). The energy scale is binding energy below the Fermi energy.

sputtered tungsten can be relied upon within our quoted uncertainties, the listed differences may not be reliable. In fact, chemical shifts this large are rarely found for atoms in ionic compounds where there is certainly a charge transfer involved.

Each strong XPS line is accompanied by two satellites. One satellite, 9.4 eV towards the Fermi energy, is a replica of the main line due to electron excitation by the 1496.0-eV Al $K\alpha_{3,4}$ radiation.[28] The second is 25 ± 1 eV away on the other side, and corresponds to primary photoelectrons which have lost energy by exciting a volume plasmon. The theoretical energy of $k=0$ free-electron plasmon is[29] $\hbar\omega_p = \hbar(4\pi ne^2/m)^{1/2}$. Bcc tungsten has six electrons per atom, two atoms per unit cell, a lattice spacing of[30] 3.16 Å, and thus a theoretical plasmon energy $\hbar\omega_p = 22.9$ eV. Fcc tungsten has six electrons per atom, four atoms per unit cell, a lattice spacing of[9] 4.15 Å, and thus a theoretical plasmon energy $\hbar\omega_p = 21.5$ eV.

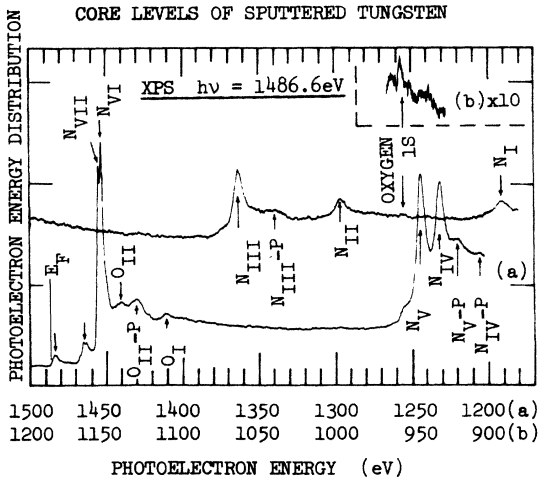

FIG. 6. Wide-scan energy distribution curves of photoelectrons excited from sputtered tungsten by Al $K\alpha_{1,2}$ x-rays. The energy scale is the measured photoelectron energy relative to the Fermi level as reference. The arrows identify the various peaks in the EDC from comparison with tabulated energies (Bearden, 1967) (Ref. 25). The inset in the upper right is part of curve (b) with ten-times higher gain. It shows a very weak signal from the oxygen 1s electrons, and thus indicates that there is very little oxygen contamination (approximately $\frac{1}{3}$ monolayer as explained in text). Any possible signal from carbon 1s electrons is hidden beneath the peak due to electrons which are excited from the tungsten N_{VI} ($4d_{3/2}$) state and subsequently lose 25-eV kinetic energy by exciting a plasmon. Arrows marked P point out the 25-eV plasmon satellites of main peaks. The curves are displaced vertically for clarity. The shape of the N_{VI}-N_{VII} doublet is distorted due to the slow response of the recorder pen. The first peak below E_F corresponds to the conduction bands. The second peak corresponds to electrons emitted from N_{VI} and N_{VII} by the weak Al $K\alpha_{3,4}$ radiation which accompanies the $K\alpha_{1,2}$ radiation.

The first experimentally determined electron energy loss spectrum[19] shows a peak at 26.8 eV although more recent experiments[20-22] give values around 23.5 eV. These values agree well with our 25-eV energy loss peaks and have been identified as volume-plasmon losses.[21] (Other smaller features have been seen, both at higher and lower energies.)

Figure 7 also shows that small oxygen contamination causes only slight broadening of the core lines and no noticeable shift of these lines. Higher contamination changes the relative strength of the observed lines in the doublet. However, the main lines of the doublet do not noticeably shift. Instead, a shoulder grows about 3.5 eV towards tighter binding from the N_{VI} peak. Thus, it appears that the shoulder is the N_{VI} line of tungsten which is chemically shifted about 3.5 eV by oxygen and carbon. The corresponding chemically shifted N_{VII} line ap-

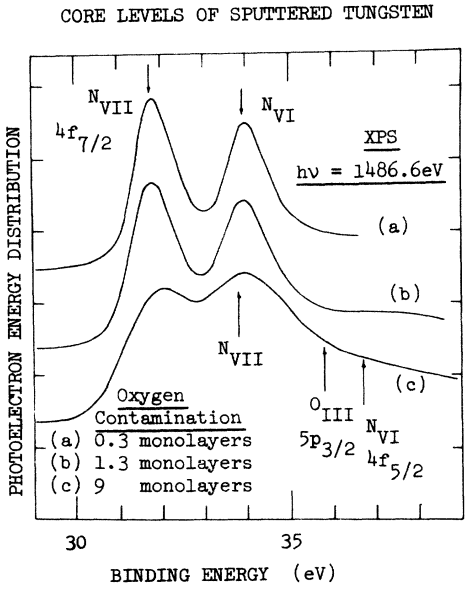

FIG. 7. Energy distribution curves for electrons excited from the N_{VI} and N_{VII} core levels of sputtered tungsten by Al $K\alpha_{1,2}$ x-rays for various levels of oxygen contamination. The downward arrows indicate our assignments for the peaks. Upward arrows indicate the energy levels as tabulated by Bearden and Burr (1967) (Ref. 25). The resolution is 1.2 eV for curves (a) and (b), and 1.5 eV for curve (c). The energy scale is photon energy minus measured photoelectron energy relative to the Fermi level as reference. For unscattered photoelectrons, this corresponds to the binding energy (below the Fermi energy) of the initially filled electron states. Curves are offset vertically for clarity. Curve (c) has different vertical sensitivity than (a) and (b).

pears somewhere under the clean tungsten N_{VI} line causing it to broaden and increase in height. Some of the general broadening of the lines is due to the use of a poorer instrumental resolution (full linewidth at half-maximum of 1.5 eV) for the contaminated sample than for the cleaner samples (1.2 eV). The lack of shift of the main lines, and the relatively small strength of the chemically shifted satellite lines on even our dirtiest samples, justifies our neglect of oxygen contamination in the XPS spectra of our cleaner samples. In Fig. 7, we also indicate the energy levels tabulated by Bearden and Burr.[25] From the positions of these levels one might be led to suspect that the data used to compile the tables may have suffered from oxygen and/or carbon contamination.

The XPS photoelectron spectrum at lower electron kinetic energies has some broad structure near 350 and near 170 eV, as shown in Fig. 8. This structure which is obscured by the rising background of secondary electrons, could correspond energetically to several possible Auger transitions.[31] Since we do not measure angular momenta of the electron states we cannot use theoretical selection rules to eliminate any of these possible transitions. The arrows indicate the most prominent structure at 166, 171, 179, and 348 eV above the Fermi energy. Harrower[19] found Auger electrons emitted at 160, 164, 173, and 340 eV above the vacuum level of electron-beam excited tungsten ribbon. His results should be increased by the work function (not specified) of his ribbon in order to refer them to the Fermi energy for comparison with our data. If we assume Harrower's ribbons had work functions of about 5 eV (see Sec. III B) then his Auger emission lines agree fairly well with ours. Others[32] have found Auger electrons at 163, 169, 179, and 350 eV above the Fermi level in polycrystalline tungsten foil; also in fairly good agreement with our present data.

TABLE I. Binding energies for crystalline tungsten tabulated by Bearden and Burr (Ref. 25), and for sputtered tungsten from our experiments. The shift, i.e., the difference between these two tabulations of core-level energy is listed in the right-hand column. See text for discussion of the reliability of these shifts.

		Crystalline tungsten binding energy (eV)	Sputtered tungsten binding energy (eV)	Shift (eV)
N_I	$4s$	595.0±0.4	594.4±1.3	0.6±1.7
N_{II}	$4p_{1/2}$	491.6±0.4	490.4±0.4	1.2±0.8
N_{III}	$4p_{3/2}$	425.3±0.4	424.0±0.4	1.3±0.8
N_{IV}	$4d_{3/2}$	258.8±0.4	256.4±0.2	2.4±0.6
N_V	$4d_{5/2}$	245.4±0.4	243.8±0.2	1.6±0.6
O_I	$5s$	77.1±0.4	76.1±1.0	1.0±1.4
O_{II}	$5p_{1/2}$	46.8±0.4	46.3±1.0	0.5±1.5
N_{VI}	$4f_{5/2}$	36.5±0.4	33.9±0.1	2.6±0.5
O_{III}	$5p_{3/2}$	35.6±0.5		
N_{VII}	$4f_{7/2}$	33.6±0.4	31.7±0.1	1.9±0.5

IV. CONCLUSIONS

We have combined ultraviolet and x-ray-induced photoelectron spectroscopy to obtain a high-resolution empirical density of state for the conduction band of sputter-deposited tungsten, that was seen to consists mostly of bcc microcrystals 10–20 Å in size. This density of states qualitatively resembles theoretical densities for crystalline tungsten, with all the fine structure greatly smoothed out. The Fermi energy of 10 eV agrees well with relativistic APW calculations of Loucks[4] and with Mattheiss's nonrelativistic APW calculations, $E_2(k)$[1], in which he used only 70% of Slater's exchange contribution to the potential. The relative merits of these two calculations are discussed by Loucks.[4]

The binding energies of the core levels have been accurately determined (some within 0.1 eV) by means of XPS measurements, calibrated by high-resolution UPS measurements. Bulk-plas-

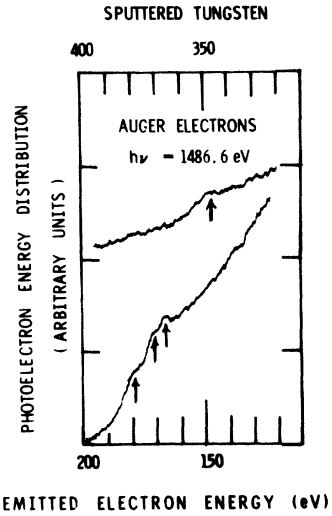

FIG. 8. Energy distribution curves of photoelectrons from sputtered tungsten excited by Al $K\alpha_{1,2}$ x-ray source ($h\nu$=1486.6 eV). The energy scale is the emitted electron energy above the Fermi level as reference. The structure in the regions near 350 and 170 eV probably corresponds to Auger transitions (see text). The curves are displaced vertically for clarity, but have the same vertical sensitivity.

mon energy losses have been observed at 25 eV.

We have seen that the effect of oxygen and carbon contamination on the photoelectron spectra of the conduction band is similar to that found for crystalline tungsten. The effect on the core-level photoelectron spectra is some general broadening and the addition of weak satellites chemically shifted by 3.5 eV to tighter binding.

ACKNOWLEDGMENTS

We wish to thank G. Krutina for aid in performing the measurements. One of us (C.M.P.) would like to thank Dr. G. Davies and Dr. M. Davies for their hospitality during his visit to King's College where the first draft of this manuscript was written.

---

*Research supported in part by the U. S. National Science Foundation and a grant from the University of Mass., Computer Center.

[1]L. F. Mattheiss, Phys. Rev. 139, A1893 (1965).
[2]T. L. Loucks, Phys. Rev. 139, A1181 (1965).
[3]T. L. Loucks, Phys. Rev. 139, A1333 (1965).
[4]T. L. Loucks, Phys. Rev. 143, 506 (1966).
[5]I. Petroff and C. R. Viswanathan, in U. S. Natl. Bur. Stand. Spec. Pub. 323, edited by L. H. Benett (U. S. GPO, Washington, D. C., 1971), p. 53.
[6]J. C. Slater, Phys. Rev. 51, 846 (1937); Phys. Rev. 81, 385 (1951).
[7]C. R. Zeisse, in Ref. 5, p. 199.
[8]J. M. Baker and D. E. Eastman, J. Vac. Sci. Technol. 10, 223 (1973).
[9]K. L. Chopra, M. R. Randlett, and R. H. Duff, Appl. Phys. Lett. 9, 402 (1966).
[10]K. L. Chopra, M. R. Randlett, and R. H. Duff, Philos. Mag. 16, 261 (1967).
[11]C. Sella and R. Coppens, C. R. Acad. Sci. B 265, 410 (1967).
[12]J. Tejeda, M. Cardona, N. J. Shevchik, D. W. Langer, and E. Schönherr, Phys. Status Solidi B 58, 189 (1973).
[13]M. Cardona, J. Tejeda, N. J. Shevchik, and D. W. Langer, Phys. Status Solidi 58, 483 (1973).
[14]A. E. Sandström, in *Handbuch der Physik*, edited by S. Flügge (Springer-Verlag, Berlin, 1957), Vol. xxx, p. 180.
[15]M. Cardona, C. M. Penchina, E. E. Koch, and P. Y. Yu, Phys. Status Solidi B 53, 327 (1972).
[16]R. D. Larrabee, Massachusetts Institute of Technology, Technical Report No. 328, 1957 (unpublished), p. 13.
[17]S. Nagata and F. Shoji, Jpn. J. Appl. Phys. 10, 11 (1971).
[18]N. J. Shevchik, J. Tejeda, and C. Cardona (unpublished).
[19]G. A. Harrower, Phys. Rev. 102, 340 (1956).
[20]C. J. Powell, J. L. Robins, and J. E. Swan, Phys. Rev. 110, 657 (1958).
[21]E. J. Scheibner and L. N. Tharp, Surf. Sci. 8, 247 (1967).
[22]D. Edwards, Jr. and F. M. Propst, J. Chem. Phys. 55, 5175 (1971).
[23]R. H. Ritchie, Phys. Rev. 106, 879 (1957).
[24]T. E. Madey and J. T. Yates, Jr., Nuovo Cimento Suppl. 5, 484 (1967).
[25]J. Bearden and A. Burr, Rev. Mod. Phys. 39, 125 (1967).
[26]B. J. Lindberg, K. Hamrin, G. Johansson, U. Gelius, A. Fahlman, C. Nordling, and K. Siegbahn, Phys. Scr. 1, 286 (1970).
[27]G. Malmsten, O. Nilsson, I. Thoren, and J-E. Bergmark, Phys. Scr. 1, 37 (1970).
[28]N. J. Shevchik, J. Tejeda, M. Cardona, and D. W. Langer, J. Phys. (to be published).
[29]C. Kittell, *Introduction to Solid State Physics*, 4th ed. (Wiley, New York, 1971).
[30]W. M. Walsh, Jr. and C. C. Grimes, Phys. Rev. Lett. 13, 23 (1964).
[31]E. H. S. Burhop, *The Auger Effect and Other Radiationless Transitions* (Cambridge U. P., Cambridge, England, 1952).
[32]P. W. Palmberg, G. E. Riach, R. E. Weber, and N. C. MacDonald, *Handbook of Auger Electron Spectroscopy* (Physical Electronics Industries Inc., Edina, Minnesota, 1972).